Tribol Lett (2016) 64:39
DOI 10.1007/s11249-016-0774-8

ORIGINAL PAPER

Analytical Friction Model of the Capsule Robot in the Small Intestine

Cheng Zhang[1] · **Hao Liu**[1]

Received: 30 July 2016 / Accepted: 14 October 2016 / Published online: 25 October 2016

Abstract One of the most important reasons that make the capsule robot cannot be used in clinic is the absence of its mechanical model, especially when the capsule robot moves at a constant velocity, which is its major working condition. An analytical friction model of the capsule robot in the small intestine is researched in the paper. The model is based on the size of the capsule robot, hyperelastic constitutive model of the small intestine's material and their interaction properties. Analytical expressions of time-dependent frictional resistance are obtained and curves are plotted when all the parameters are substituted. Compared with experimental results, the model calculation results are valid. The errors of the period, valley value and peak value are 6.88, 9.38 and 4.78 %, respectively. The work is hoped to perfect the friction model between the capsule robot and the small intestine and contribute to the development of the capsule robot.

Keywords Biotribology · Capsule robot · Intestine · Analytical model · Hyperelasticity

1 Introduction

The morbidity of gastrointestinal disease is increasing with faster pace of life and more aging population in the worldwide, especially that of the tumor, bleeding and dysfunction in the intestine. Capsule endoscopy (CE) and enteroscope are the main methods in the intestinal disease diagnosis, among which the former is more effective [1–3]. The only absolute contraindication of CE diagnosis is ileus, because CE used in clinic moves with intestinal peristalsis [4]. A kind of active capsule robot (CR) can solve this problem, but it is still at the stage of laboratory research because of the problems of drive, control, power supply and so on. Now the drive methods of CR contain external drive such as magnetic drive [5–8] and internal drive such as bionic drive [9–11] and hybrid drive [12, 13]. Uniform motion is an important working condition for all of these drive methods, especially for the magnetic drive, which may be the closest approach to clinical application.

More and more researchers are aware that the intestinal tribological properties may result in inefficient or inadequate CR system. Quantification of frictional resistance of the intestine to assist with developing CR has been an area of research since 2000 [14]. In the same year, wireless capsule endoscopy was developed by Given Imaging Ltd. [15]. The factors that influence frictional resistance most are the material property of the intestine and the parameters of the CR. Ciarletta et al. [16] described the material of the intestine with a hyperelastic model. Woo et al. [17] regarded the intestinal wall as a thin wall and used Stokes' drag equation. Kim et al. [18] used the viscoelasticity model and built a five-element model to present the viscoelastic property of stress relaxation. Every model has its own advantage and should be used in accordance with specific conditions. The friction resistance can also be influenced by CR's parameters, such as weight [19], shape [20], dimension [21], material [22], contour line and surface preparation methods [23]. Furthermore, the velocity of CR was proved to affect the friction resistance when CR moves in the intestine. Kim et al. [24] obtained a qualitative result that the friction goes up with the velocity

✉ Hao Liu
liuhao@sia.cn

[1] State Key Laboratory of Robotics, Shenyang Institute of Automation (SIA), Chinese Academy of Sciences, Shenyang 110016, China

increasing by experiment. My previous work also shows the same result [25, 26, 27], and we analyzed the friction resistance of CR at stage of start, stop and uniform motion [28]. It is found that the friction exhibits fluctuating change when CR moves at a constant velocity, which has a great significance for the control strategy of CR [29]. But the absence of analytical model results in that it cannot be used directly.

Analytical friction model of the capsule robot in the small intestine is studied in the paper. A classic shape of capsule is chosen for the research, because the resistance of CR is hoped to be lowest when it moves. The material property of the small intestine is represented by an anisotropic hyperelastic model. The geometric model of the interaction between CR and the small intestine is simplified based on truth. An analytical model is developed according to the phenomenon of fluctuating friction, constitution of frictional resistance and material property of the small intestine. The model is related to the size and the velocity of CR. The validity of the model will be verified by experiment. The result of this work is hoped to be used for the development of the control strategy of CR.

2 Interaction Between CR and Intestine

The interaction between CR and the small intestine is analyzed in this section, which contains the geometric relationship and the interaction force. A reasonable shape of CR is chosen according to the actual application. The material property of the small intestine is chosen according to its deformation and deformation rate.

2.1 Shape and Size of CR

A classic shape of capsule is used in this model, which has been proved to be of least resistance [30]. As shown in Fig. 1, the center of CR is a cylinder and both of the two ends are hemispheroids. They have the same radius R, and the height of the cylinder is L. CR is hoped to be small and with a low resistance when it moves. Most of the magnetic drive CRs use this kind of shape. CR with external drive mechanisms always does its best to draw back them when moving. Therefore, it is reasonable and universal to choose the shape to study in the model.

Fig. 1 Shape and size of CR

2.2 Material Property of the Small Intestine

The main work environment of CR is the small intestine, which can be seen as a soft tube, full of twists and turns. It brings many difficulties to the motion of CR. Actually, the small intestine is not a homogeneous material, the outer layer of which is muscle layer and the inner layer is mucous layer. Research shows that the muscle layer exhibits hyperelasticity, while the mucous layer exhibits viscoelasticity. Moreover, each of the two layers is anisotropic [31]. The small intestinal peristalsis always happens in vivo. We regard the small intestine as a straight soft tube, not layered, in order to simplify the model. The intestinal peristalsis also is not taken into account.

The material of the whole small intestine has viscoelastic and hyperelastic characteristics simultaneously because of the layered structure of the small intestine. The time response of the material can be described by the viscoelasticity, such as stress relaxation and creep. The viscoelastic property is obvious in the case of large deformation analysis. If CR continuously moves in the small intestine, the small intestine stretches and retracts with it. The mucous layer plays the leading role for the smaller deformation caused by CR, but the muscle layer also deforms, because the small intestine is a whole. The time response is not obvious, and the hyperelastic characteristics become more distinct under the circumstances. Therefore, the hyperelastic theory of the intestine is used in this paper to reproduce its purely elastic passive response from the structural organization of its main constituents [16]. The analytic expressions of the hyperelastic constitutive model that shows the stress–strain relationship of the material in the longitudinal and circumferential directions are given by

$$\begin{aligned}\sigma_l = {} & c_1 \cdot \left(1 - \frac{1}{\lambda_1^4}\right) \\ & + \frac{3\lambda_1^4 - 1}{2\lambda_1^4} \cdot k_{1Coll} \cdot (I_1 - 1)\left[e^{k_{2Coll}(I_1-1)^2}\right] \\ & + k_{1LM} \cdot \left(\lambda_1^2 - 1\right)\left[e^{k_{2LM}\left(\lambda_1^2-1\right)^2}\right]\end{aligned} \tag{1}$$

and

$$\begin{aligned}\sigma_c = {} & c_1 \cdot \left(1 - \frac{1}{\lambda_2^4}\right) \\ & + \frac{\lambda_2^4 - 3}{2\lambda_2^4} \cdot k_{1Coll} \cdot (I_2 - 1)\left[e^{k_{2Coll}(I_2-1)^2}\right] \\ & + k_{1CM} \cdot \left(\lambda_2^2 - 1\right)\left[e^{k_{2CM}\left(\lambda_2^2-1\right)^2}\right]\end{aligned} \tag{2}$$

where

$$I_1 = \frac{3\lambda_1^4 + 1}{4\lambda_1^2}; \quad I_2 = \frac{\lambda_2^4 + 3}{4\lambda_2^2} \tag{3}$$

λ_1 and λ_2 are the principal stretches in the longitudinal and circumferential directions, respectively. c_1 is a constant material parameter. k_{1Coll}, k_{2Coll} are two material parameters describing the stiffening properties of the collagen network. (k_{1LM}, k_{2LM}) and (k_{1CM}, k_{2CM}) are the material parameters accounting for the exponential increase in stress with stretch ratio due to the longitudinal and circular muscle layers, respectively. Equations (1) and (2) are expressed as

$$\begin{aligned} \sigma_l &= H_l(\lambda_1) \\ \sigma_c &= H_c(\lambda_2) \end{aligned} \tag{4}$$

for simplification.

2.3 Interaction Model Between CR and Intestine

The interaction model, which contains the geometric model and the mechanical model, has a significant influence on the accuracy of the analytical friction model. It is required not only to approach to reality, but also to be simple enough for the analytic calculation. When CR moves inside, the small intestine is forced to expand. Based on this, the geometric model between CR and intestine is shown in Fig. 2. The central angle corresponding to the connection area between the front end of CR and the small intestine is α. CR is wrapped up by the small intestine except part of its ends, and the whole geometrical shape is axisymmetric. The mechanical model is also shown in Fig. 2. CR is forced to move with a constant velocity v_c. d and D are the average wall thickness and inner diameter of the small intestine. The interactive force of CR contains the friction f and the circumferential pressure P. The direction of the former is opposite to CR's moving direction, while that of the latter is perpendicular to CR's shell. The contact pressure on the tail end is neglected.

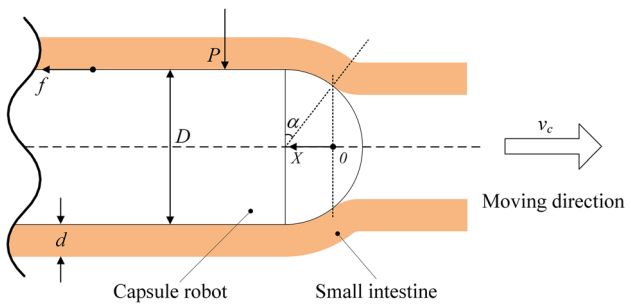

Fig. 2 Interaction model between CR and intestine

For further development of the model, the following assumptions are made.

1. The material of the small intestine is incompressible.
2. The small intestine deforms symmetrically toward its radial direction and its cross-sectional area is constant.
3. The deformation of the small intestine is the same as the external shape of the contact surface of CR.
4. The small intestine deforms at a constant velocity.

3 Analytical Model of the Fluctuant Friction

It has been proved that the friction of CR is fluctuant when CR moves in the small intestine with a constant velocity. The whole process can be simplified to a simple physical model, which is shown in Fig. 3 [29]. An infinitely long flat car is placed on a smooth surface. One side of the car is connected to the wall by a nonideal spring, which may be nonlinear and include dampers. A slider is placed on the flat car. The friction between them is f. The slider moves at v_c. The spring is used to express the stain and stress of the small intestine in the longitudinal direction, while the friction f represents the frictional resistance between CR and the small intestine. The immediate cause is that the relative sliding between CR and the small intestine appears periodically. That is to say, relatively static state and relative motion alternate periodically when CR moves. The root cause is that the small intestine is a soft tube, whose material is anisotropic and hyperelastic. When CR moves, the small intestine resists it; meanwhile, the small intestine stretches. The critical condition of the relative motion is the frictional resistance between CR and the small intestine that equals the tension resulted from the stretch of the small intestine. Therefore, relatively static state and relative motion should be analyzed separately.

3.1 Relatively Static State

There is no relative sliding between CR and the small intestine in the relatively static state. More precisely, no relative sliding occurs on the front end of CR, but the small intestine may be stretched or in the initial state. When the

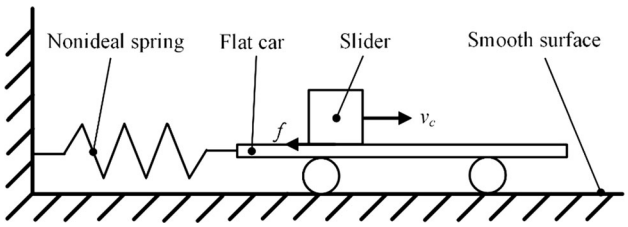

Fig. 3 Equivalent physical model

resistance is smaller than the tension of the small intestine, the relative sliding occurs. According to the force analysis in Fig. 2, the frictional resistance F of CR can be expressed as

$$F = F_e + f_v + f_c \tag{5}$$

where F_e is the environmental resistance, f_v is the viscous friction, and f_c is the Coulomb friction.

Environmental resistance is the horizontal component of the circumferential pressure on the front end of CR. The environmental resistance applied at the rear of the capsule is neglected.

$$F_e = \int_0^{R\sin\alpha} 2\pi RP(x)\mathrm{d}x \cdot \sin\alpha \tag{6}$$

where $P(x)$ is the circumferential pressure at position x, which can be expressed as [25]

$$P(x) = \frac{2dH_c(\lambda_2(x))}{D(x)} \tag{7}$$

Viscous resistance is the product of the relative velocity and the apparent viscosity coefficient. So it equals zero in the condition of static friction.

Coulomb friction is decided by the local contact pressure and the Coulomb friction coefficient (COF).

$$\begin{aligned} f_c &= \mu N \\ &= \mu\left[\int_0^{R\sin\alpha} 2\pi RP(x)\mathrm{d}x \cdot \cos\alpha + 2\pi RLP_m\right] \end{aligned} \tag{8}$$

$$P_m = \frac{2dH_c\left(\frac{D}{2R\cos\alpha}\right)}{D} \tag{9}$$

where μ is the COF and N is the local contact pressure. The first term of N is circumferential pressure on the front end and the second is that on the middle cylinder.

In the initial state, no stretch of the small intestine occurs and the frictional resistance of CR is the environmental resistance.

$$F_{\text{initial}} = F_e \tag{10}$$

Under the critical condition, the frictional resistance is maximal, which equals the tension of the small intestine.

$$F_{critical} = F_e + f_c \tag{11}$$

The reason why the resistance increases is that the small intestine is stretched. Therefore, the numerical value of resistance increasing can be equivalent to the tension of the small intestine. According to the stress–strain relationship of the material in the longitudinal direction, the tension T can be expressed as

$$\begin{aligned} T &= \sigma_l \cdot s \\ &= H_l\left(\lambda_1\left(\frac{v_c t}{L}\right)\right) \cdot \pi\left(2Rd + d^2\right) \end{aligned} \tag{12}$$

where s is the sectional area of the small intestine in the section of the middle of CR, t is the time. The time-varying friction resistance of CR is

$$F = F_{\text{initial}} + T \tag{13}$$

The maximal of F is $F_{critical}$ under the critical condition. After that, the relatively static state is over and the relative motion begins.

3.2 Relative Motion

When the tension of the small intestine is larger than the frictional resistance of CR, the friction converts from static friction to sliding friction. The friction of CR is same as the tension of the small intestine, because CR moves in a constant velocity. The relative velocity v is

$$v = v_c + v_i \tag{14}$$

where v_i is the contraction speed. If the system of CR and the small intestine is regarded as a spring oscillator, the system is in an overdamping state in free vibration [32]. That is to say, CR returns to the equilibrium position slowly without vibration. Therefore, it is assumed that the small intestine contracts to its initial state in relative motion. In a real-world situation, the contraction speed variates change nonlinearly. In the paper, it is taken as an average for simplification. The time-varying friction resistance of CR in relative motion is:

$$F = F_{\text{critical}} - T' \tag{15}$$

$$T' = H_l\left(\lambda_1\left(\frac{vt}{L}\right)\right) \cdot \pi\left(2Rd + d^2\right) + f_v \tag{16}$$

The friction resistance contains environmental resistance and viscous friction in the relative motion. Above all, the frictional resistance is fluctuant between F_{initial} and F_{critical} when CR moves in the small intestine with a constant velocity. Their relative motion is shown as a stick–slip motion. The schematic diagram of the frictional resistance and relative velocity of three periods is shown in Fig. 4.

4 Model Verification

4.1 Parameters of the Model

According to the analytical model above, the model's calculating results are compared to the experimental results to test the model accuracy. All the measurable and known

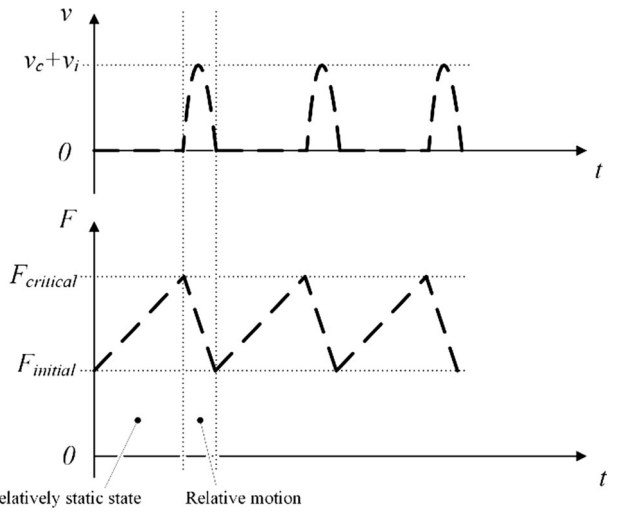

Fig. 4 Schematic diagram of the frictional resistance and relative velocity

parameters are shown in Table 1. The parameters of the hyperelastic constitutive model are taken from Ciarletta's work [16]. The size of CR is the same as the dummy used in the experiment. The measured inner diameter of the jejunum section is about 9 mm in the relaxed state. So the central angle corresponding to the connection area between the front end of CR and the small intestine α is 30° in calculation. Lyle [33] measured mean COF in their work. It has been proved that COF between CR and the small intestine mainly depends on the material of CR and the bowel region. The polydimethylsiloxane (PDMS) is a kind of inert and innoxious material, which is also used in commercialized CE. Therefore, a PDMS capsule dummy and the jejunum section of the small intestine are used in the verification experiment and $\mu = 0.015$ is used in the paper according to Lyle's conclusion. The experiment results show that the fluctuation change disappears when CR moves fast. The velocity of CR is 0.5 mm/s in the experiment. The average speed of contraction of the small intestines is 0.6 mm/s by calculation [32]. Viscous friction is related to the relative velocity, which was analyzed in my previous work. The result shows that the viscous friction at 0.5 mm/s is 0.74 mN [25]. Compared with F_{critical}, f_v is so small that it can be neglected in the calculation.

Substituting the parameters above to Eqs. (10) and (11), we obtain the frictional resistances in the initial and critical state.

$$\begin{aligned} F_{\text{initial}} &= 23.23 \text{ mN} \\ F_{\text{critical}} &= 39.79 \text{ mN} \end{aligned} \tag{17}$$

Substituting the parameters in Table 1 to Eqs. (13) and (15), we obtain the analytical functions of the friction changing with time and plot the curves in Figs. 5 and 6, respectively. The numeric expressions are

$$\begin{aligned} F_{\text{increasing}} = {} & 264.1(m_i - 1)e^{0.84(m_i-1)^2} - \frac{192.2}{m_i^2} \\ & + 1339m_i^2\left(3m_i^2 - 1\right)J_i e^{12.01J_i^2} + 215.5 \end{aligned} \tag{18}$$

$$\begin{aligned} F_{decreasing} = {} & -264.1(m_d - 1)e^{0.84(m_d-1)^2} + \frac{192.2}{m_d^2} \\ & - 1339m_d^2\left(3m_d^2 - 1\right)J_d e^{12.01J_d^2} \end{aligned} \tag{19}$$

where

$$\begin{aligned} J_i &= 0.75m_i^3 + 0.25m_i - 1 \\ J_d &= 0.75m_d^3 + 0.25m_d - 1 \\ m_i &= (0.01887t + 1)^2 \\ m_d &= (0.04151t + 1)^2 \end{aligned} \tag{20}$$

It takes about 0.059 s to increase from initial state to critical state in the increasing process, while about 0.0268 s is used in the decreasing time. The friction fluctuation in three periods is shown in Fig. 7. The period of the fluctuation is 0.0858 s.

Table 1 Certain parameters in the model

c_1	1.58 kPa
k_{1Coll}	22.01 kPa
k_{2Coll}	12.1
k_{1CM}	77.12 kPa
k_{2CM}	0.516
k_{1LM}	2.17 kPa
k_{2LM}	0.84
R	6.5 mm
L	20 mm
d	2.5 mm
μ	0.015
α	30°
v_c	0.5 mm/s
v_i	0.6 mm/s

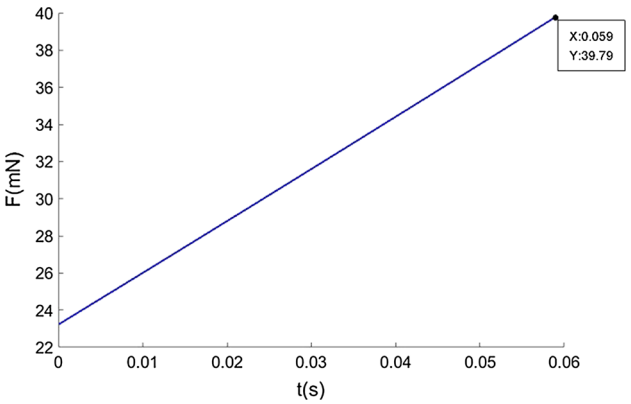

Fig. 5 Process of the friction increasing with time

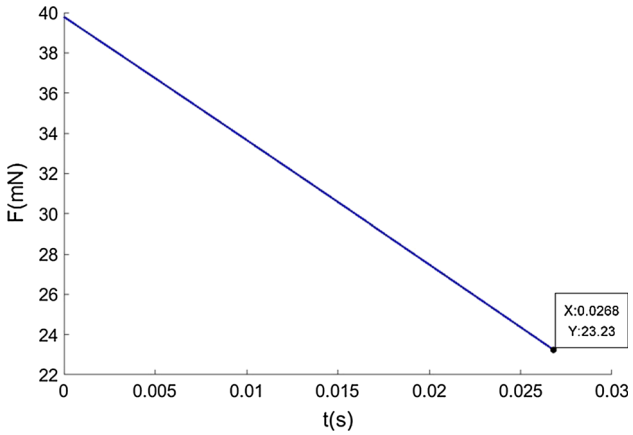

Fig. 6 Process of the friction decreasing with time

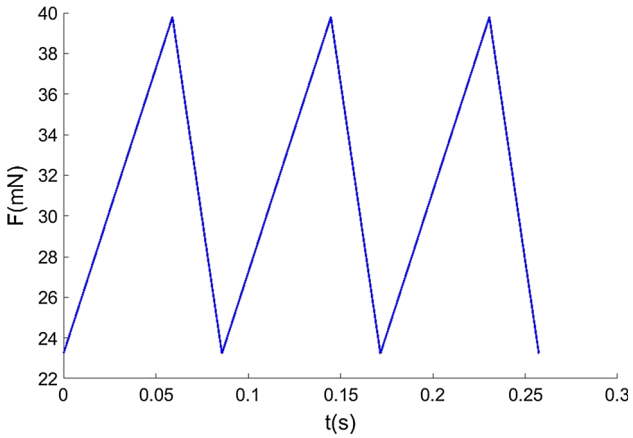

Fig. 7 Friction fluctuation in three periods

4.2 Experiment Validation

A homemade uniaxial experiment platform was developed to test the friction change in the starting process. It consists of two parts: drive unit and data acquisition unit; see Fig. 8. The main part of the drive unit is LMX1E series linear motor system, which is produced by HIWIN. The positioning accuracy of the system can reach ±1 μm. The left side of the drive unit is load platform. The rotor of the linear motor is combined with a support, on which a single freedom-degree micro-force sensor (FUTEK LSB200) is fixed. The probe of the force sensor is connected to a capsule that is placed inside the intestine with polymer string. In order to simulate the environment where the intestine locates in vivo, we use flexible polyurethane foam (PUF) as the basement, which is fixed on the load platform. PCI 6229 data acquisition (DAQ) card produced by NI is used to acquire the voltage signal of encoder and micro-force sensor. Then the signal is transmitted to computer for saving and analysis.

The jejunum section of the small intestine used in the experiment was taken from a standardized laboratory pig to ensure the repeatability of experimental results. In order to reduce the effect of the food debris within the intestine, the pig was kept off food, but not water for 24 h. Under the supervision of the medical ethics committee, the pig was killed with an anesthetic overdose and anatomized by professionals. Segments of jejunum were excised from the pig immediately following euthanization and stored in a slot that is filled with 37 °C Tyrode's solution with continual oxygen supply (1000 ml Tyrode's solution consists: NaCl 8.0 g, KCl 0.2 g, $MgSO_4.7H_2O$ 0.26 g, $NaH_2PO_4.2H_2O$ 0.065 g, $NaHCO_3$ 1.0 g, $CaCL_2$ 0.2 g, glucose 1.0 g). When exposed to unconditioned air, intestinal tissue drying had been observed and previously remedied by applying saline to the tissue surface. Because of lack of constant temperature and humidity system in the experiment platform, the way of frequent same type test specimens changing is adopted to ensure the mechanical property of the test specimen. The mesentery and one side of the intestine specimen are fixed on the basement.

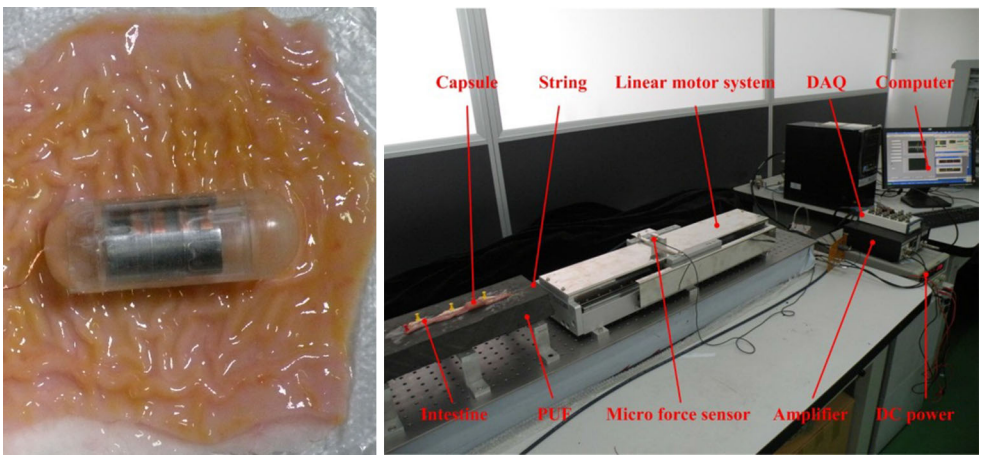

Fig. 8 PDMS CR dummy and experiment platform for measuring frictional change

The PDMS CR dummy is forced to move at 0.5 mm/s in the small intestine. The frictional resistance of CR is shown in Fig. 9. CR moves from static to uniform motion. Meanwhile, friction resistance increases from 0 to a stable value. When CR moves in a constant velocity after 0.3 s, it is obvious that the friction resistance fluctuates. Eight periods of fluctuating curve are chosen to compare with the model calculation results. The period, valley value and peak value of every period of the experimental results are listed in Table 2 based on the red mark points. The deviations of them between the averages of the experimental results and the model calculation results are 6.29, 2.37 and 11.81 %, respectively .

The experiment is repeated using the same section of jejunum. The frictional resistance of CR is shown in Fig. 10. The experiment is repeated using a different section of jejunum again. The frictional resistance is shown in Fig. 11. The data before 1.2 s appear obvious anomalous change, so it cannot be used in the analyses. According to the data in 30 periods in three times experiment, the distributions of the period, valley value and peak value are shown in Fig. 12. The red-dotted lines in the picture are the positions of the model calculation results. The theoretical results of period and valley value are in or beside the areas of maximum weight. But there is deviation in the peak value results. The errors of all the data between the averages of the experimental results and the model calculation results are 6.88, 9.38 and 4.78 %, respectively. In conclusion, the analytical friction model can predict the frictional resistance of CR moving in the small intestine effectively.

5 Discussion

5.1 Influence of CR's Velocity

We have found that CR's velocity has an effect on the frictional resistance. Their function relationship is explained detailedly in our previous work [25]. F_{initial} and F_{critical} are constant in the analytical model. That is to say, the amplitude of the fluctuation has nothing to do with CR's velocity. Frictional resistance at 0.5 mm/s is

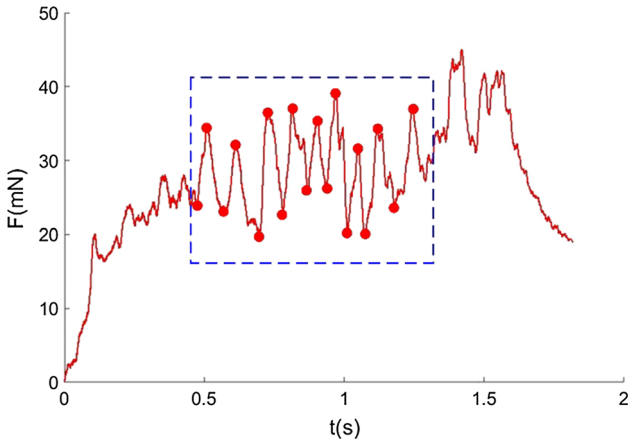

Fig. 9 Frictional resistance of CR at 0.5 mm/s

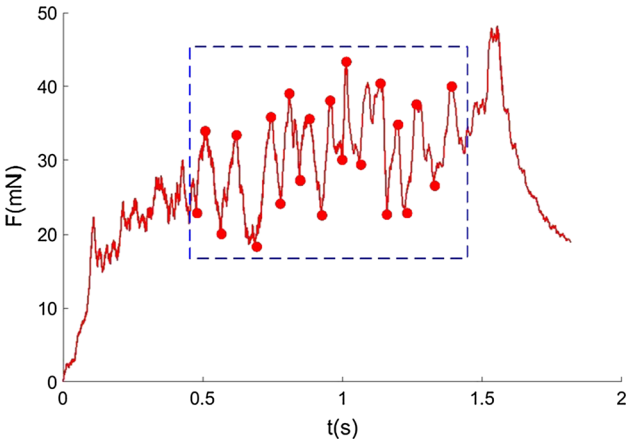

Fig. 10 Repeated experiment result with the same jejunum specimen

Table 2 Details of the results

	Period (s)	Valley value (mN)	Peak value (mN)
Period 1	0.1001	23.85	34.45
Period 2	0.1168	22.85	32.03
Period 3	0.0848	19.51	36.59
Period 4	0.0877	22.66	36.99
Period 5	0.0629	25.99	35.37
Period 6	0.0862	26.34	39.31
Period 7	0.063	20.13	31.68
Period 8	0.128	20.12	34.27
Average of experimental results	0.0912	22.68	35.09
Model calculation results	0.0858	23.23	39.79
Deviations	6.29 %	2.37 %	11.81 %

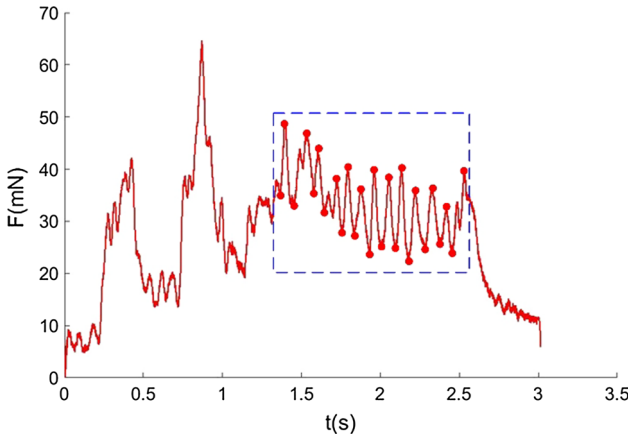

Fig. 11 Repeated experiment result with a different section of jejunum specimen

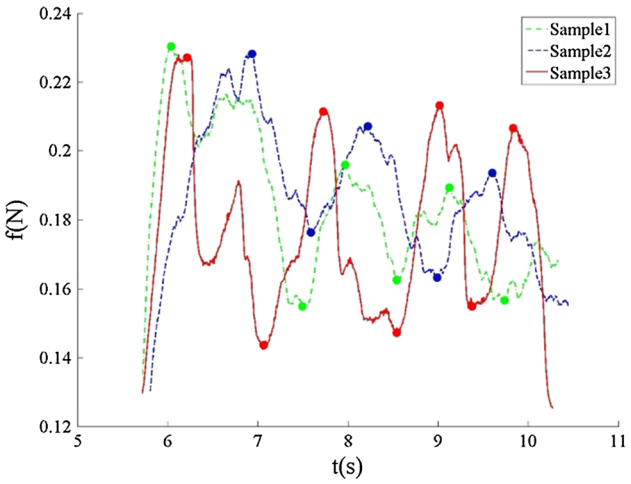

Fig. 13 Repetitive experimental data at 10 mm/s [29]

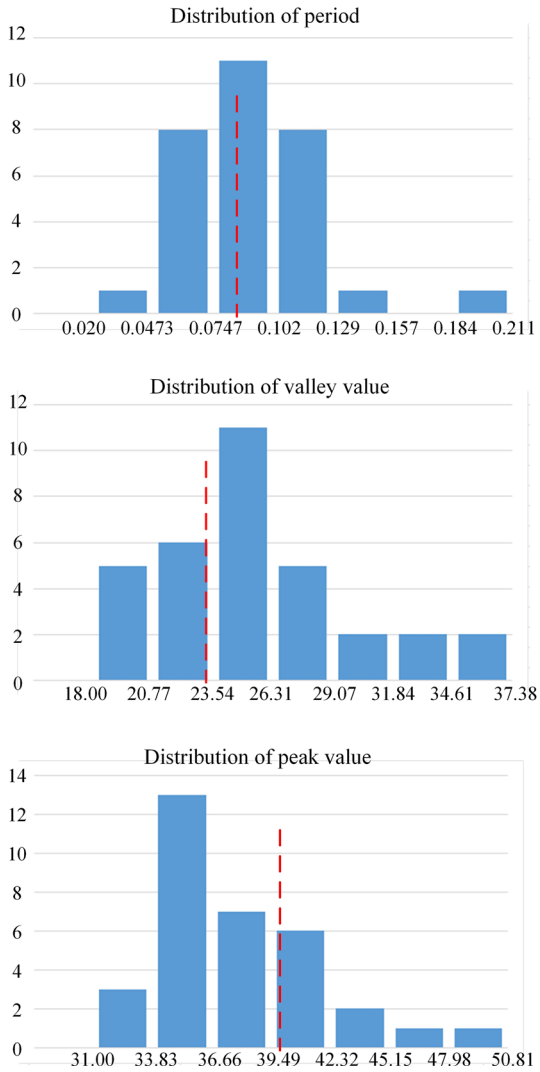

Fig. 12 Distribution of period, valley value and peak value

approximately equal to the mean value of the fluctuant resistance in the model. So CR moving at 0.5 mm/s is chosen as the confirmatory experiment. But it is impossible to ignore that the friction fluctuation exists when CR moves in the small intestine at a lower velocity. For example, when CR moves at 10 mm/s, the repetitive experimental results are shown in Fig. 13. F_{initial} and F_{critical} are 140 and 194 mN approximately under the circumstances. Compared with the friction at 0.5 mm/s, the results agree with the conclusion that the friction of CR increases with its velocity. But the model in the paper cannot describe the friction at 10 mm/s.

The main reason is hyperelastic constitutive model that is used to describe the material of the small intestine in the model. Time parameter is not contained in the hyperelastic constitutive model. It results from the absence of the influence of CR's velocity. Therefore, the analytical model in the paper only can be used when CR moves at 0.5 mm/s. The material of the small intestine has viscoelastic and hyperelastic characteristics. If the model needs to be perfected to apply to all the velocity section, a more reasonable material model of the small intestine is need in the future. We are thinking about using the hyperelastic and viscoelastic constitutive model to express the longitudinal and circumferential directions, respectively, because the time response is more obvious in the circumferential direction. But the coupling relationship of the two directions needs to be further studied.

5.2 Influence of COF

As an important parameter for the research of CR's friction, COF has an effect on the Coulomb friction directly. The COF for the small intestine in contact with another

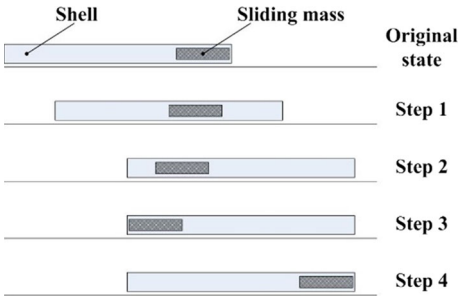

Fig. 14 Driving principle of the vibro-impact CR

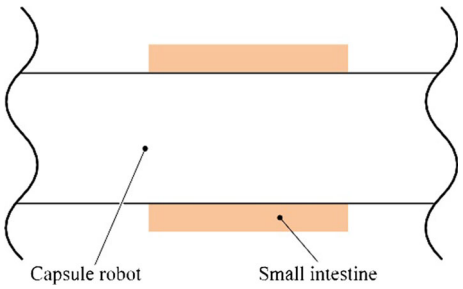

Fig. 15 Interaction between CR and the small intestine without regard to boundary conditions

surface is highly variable and depends upon the surface material, region of intestine, contact area and animal [33]. The surface material is PDMS, and the experiment object is laboratory pig in my work. The contact area depends on the size of CR. On these conditions, COF ranges from 0.008 to 0.018 in different parts of the small intestine. The corresponding F_{critical} ranges from 32.06 to 43.1 mN. The peak value of friction fluctuation has a deviation range in the whole small intestine. This is only a theoretical result, which needs further experimental validation.

5.3 Research Significance for the Vibro-Impact CR

Vibro-impact drive mode is one kind of internal drive. Vibro-impact CR consists of a capsule main body (shell) interacting with a harmonically driven internal mass [34, 35, 36], which is shown in Fig. 14. It relies on internal force and external static friction to move itself forward and backward. But it nearly cannot move inside the intestine, because the resistance from the circumferential deformation of the intestine is larger; what is more, the deformation in the longitudinal direction nearly counteracts the external static friction of CR. Several methods are taken into account to solve the problem. One of them is increasing the frequency of the reciprocating motion of CR's internal mass. According to experimental result, the small intestine recovers in about 0.05 s after it is forced to extend. If the motion period of the vibro-impact CR is less than 0.05 s, the next motion period begins before the small intestine recovers. Under the circumstances, displacement of CR will be accumulated before the contraction of the intestine. When the accumulated displacement is larger than the intestine's stretch, relative slip between CR and the intestine occurs. It is impossible that the displacement in single period is larger than the extension of the small intestine, because the length and the internal force of the vibro-impact CR are limited.

5.4 Equivalent Physical Model

The traditional physical model of stick–slip motion is a mass attached to a coiled spring being pulled by a tension force so that the spring moves at a constant velocity [37]. The process that CR moves in the small intestine can be regarded as a specific form of stick–slip motion according to the curves of the frictional resistance and relative velocity. The physical model shown in Fig. 3 should be verified further because many preconditions are assumptive. For example, the small intestines at the front end and the middle section are inconsecutive, the stretch of the small intestine only appears at the middle section. The primary cause of these problems is the boundary conditions. The interaction relationship can be simplified to Fig. 15 if the boundary conditions are neglected. The friction induced by circumferential stress on the premise of relative static state is the only resistance that hinders CR moving. Meanwhile, the section of the small intestine is forced to stretch. This equivalent model can simplify the relation between CR and the small intestine without regard to boundary conditions. After substituting the constitutive equations of the small intestine to the model, we can get the analytical expression of the frictional resistance. Different constitutive equations in different directions can be used conveniently. Although the simplification has no practical significance, the confirmatory experiment and data acquisition are easy to be implemented. If the equivalent physical model is proved to be available, it will be a new research method for the instrument in a soft tube.

6 Conclusion

An analytical friction model of the capsule robot in the small intestine is developed in the paper based on the small intestine's anisotropic hyperelastic constitutive model and their geometrical and force relationship. The friction changing is divided to two sections: relatively static state and relative motion. The analytical expressions of friction at initial state, critical state and changing process are deduced. Substituting the measurable and known parameters to the expressions, we get the curves of friction changing. The model is validated by experimental results. The deviations of the period, valley value and peak value are 6.88, 9.38 and

4.78 %, respectively. The equivalent physical model is significant for the research of friction between CR and the small intestine. But a more reasonable material constitutive model is needed to perfect it. This work is hoped to be used to optimize the CR's control method.

Acknowledgments This work was supported by the National Natural Science Foundation of China (No. 61503370), National Science and technology support program (2015BAI01B13) and the Natural Science Foundation of Liaoning Province (No. 20141151).

References

1. Dionisio, P.M., Gurudu, S.R., Leighton, J.A., Leontiadis, G.I., Fleischer, D.E., Hara, A.K., Heigh, R.I., Shiff, A.D., Sharma, V.K.: Capsule endoscopy has a significantly higher diagnostic yield in patients with suspected and established small-bowel Crohn's disease: a meta-analysis. Am. J. Gastroenterol. **105**(6), 1240–1248 (2010)
2. Goenka, M.K., Majumder, S., Kumar, S., Sethy, P.K., Goenka, U.: Single center experience of capsule endoscopy in patients with obscure gastrointestinal bleeding. World J. Gastroenterol **17**(6), 774–778 (2011)
3. Lepileur, L., Dray, X., Antonietti, M., Iwanicki-Caron, I., Grigioni, S., Chaput, U., Di-Fiore, A., Alhameedi, R., Marteau, P., Ducrotte, P., Lecleire, S.: Factors associated with diagnosis of obscure gastrointestinal bleeding by video capsule enteroscopy. Clin. Gastroenterol. H **10**(12), 1376–1380 (2012)
4. Sidhu, R., Sanders, D.S., Morris, A.J., McAlindon, M.E.: Guidelines on small bowel enteroscopy and capsule endoscopy in adults. Gut **57**(1), 125–136 (2008)
5. Rahman, I., Pioche, M., Shim, C.S., Lee, S.P., Sung, I.K., Saurin, J.C., Patel, P.: Magnetic-assisted capsule endoscopy in the upper GI tract by using a novel navigation system. Gastrointest. Endosc. **83**(5), 889-U866 (2016)
6. Yongshun, Z., Dianlong, W., Dongming, G., Honghai, Y.: Characteristics of magnetic torque of a capsule micro robot applied in intestine. IEEE Trans. Magn. **45**(5), 2128–2135 (2009)
7. Cancheng, Z., Chao, H., Fei, L.: Open-loop control experiment of wireless capsule endoscope based on magnetic field. In: 2011 IEEE International Conference on Information and Automation (ICIA), 6–8 June 2011, pp. 51–56
8. Floyd, S., Pawashe, C., Sitti, M.: An untethered magnetically actuated micro-robot capable of motion on arbitrary surfaces. In: 2008 IEEE International Conference on Robotics and Automation, 19–23 May 2008, pp. 419–424
9. Wang, K., Wang, Z., Zhou, Y., Yan, G.: Squirm robot with full bellow skin for colonoscopy. In: 2010 IEEE International Conference on Robotics and Biomimetics (ROBIO), 14–18 Dec 2010, pp. 53–57
10. Valdastri, P., Webster, R.J., Quaglia, C., Quirini, M., Menciassi, A., Dario, P.: A new mechanism for mesoscale legged locomotion in compliant tubular environments. IEEE Trans. Robot. **25**(5), 1047–1057 (2009)
11. Wang, X.N., Meng, M.Q.H.: An inchworm-like locomotion mechanism based on magnetic actuator for active capsule endoscope. In: 2006 IEEE/RSJ International Conference on Intelligent Robots and Systems, 9–15 Oct 2006, pp. 1267–1272
12. Simi, M., Valdastri, P., Quaglia, C., Menciassi, A., Dario, P.: Design, fabrication, and testing of a capsule with hybrid locomotion for gastrointestinal tract exploration. IEEE/ASME Trans. Mechatron. **15**(2), 170–180 (2009)
13. Wang, X.N., Meng, Q.H., Chen, X.J.: A locomotion mechanism with external magnetic guidance for active capsule endoscope. In: 2010 Annual International Conference of the IEEE Engineering in Medicine and Biology Society (EMBC), Aug 31–Sept 4 2010, pp. 4375–4378
14. Hoeg, H.D., Slatkin, A.B., Burdick, J.W., Grundfest, W.S.: Biomechanical modeling of the small intestine as required for the design and operation of a robotic endoscope. In: Proceedings of IEEE International Conference on Robotics and Automation, 24–28 Apr 2000, pp. 1599–1606
15. Iddan, G., Meron, G., Glukhovsky, A., Swain, P.: Wireless capsule endoscopy. Nature **405**(6785), 417 (2000)
16. Ciarletta, P., Dario, P., Tendick, F., Micera, S.: Hyperelastic model of anisotropic fiber reinforcements within intestinal walls for applications in medical robotics. Int. J. Robot. Res. **28**(10), 1279–1288 (2009)
17. Woo, S.H., Kim, T.W., Mohy-Ud-Din, Z., Park, I.Y., Cho, J.-H.: Small intestinal model for electrically propelled capsule endoscopy. BioMed. Eng. Online **10**(108), 1–20 (2011)
18. Kim, J.S., Sung, I.H., Kim, Y.T., Kim, D.E., Jang, Y.H.: Analytical model development for the prediction of the frictional resistance of a capsule endoscope inside an intestine. Proc. Inst. Mech. Eng. Part H-J. Eng. Med. **221**(H8), 837–845 (2007)
19. Zhang, C., Su, G., Tan, R., Li, H.: Experimental investigation of the intestine's friction characteristic based on "internal force-static friction" capsubot. In: Proceedings of the 8th IASTED International Conference on Biomedical Engineering, 12–18 Feb 2011, pp. 117–123
20. Wang, K.D., Yan, G.Z.: Research on measurement and modeling of the gastro intestine's frictional characteristics. Meas. Sci. Technol. **20**(1), 1–6 (2009)
21. Wang, X., Meng, M.Q.H.: An experimental study of resistant properties of the small intestine for an active capsule endoscope. Proc. Inst. Mech. Eng. Part H-J. Eng. Med. **224**(H1), 107–118 (2010)
22. Li, J., Huang, P., Luo, H.D.: Experimental study on friction of micro machines sliding in animal intestines. Run Hua Yu Mi Feng/Lubr. Eng. **175**(3), 119–122 (2006)
23. Sliker, L.J., Wang, X., Schoen, J.A., Rentschler, M.E.: Micropatterned treads for in vivo robotic mobility. J. Med. Devices-Trans. ASME **4**(4), 041006 1-8 (2010)
24. Kim, J.S., Sung, I.H., Kim, Y.T., Kwon, E.Y., Kim, D.E., Jang, Y.H.: Experimental investigation of frictional and viscoelastic properties of intestine for microendoscope application. Tribol. Lett. **22**(2), 143–149 (2006)
25. Zhang, C., Liu, H., Tan, R.J., Li, H.Y.: Modeling of velocity-dependent frictional resistance of a capsule robot inside an intestine. Tribol. Lett. **47**(2), 295–301 (2012)
26. Zhang, C., Liu, H., Tan, R.J., Li, H.Y.: Interaction model between capsule robot and intestine based on nonlinear viscoelasticity. Proc. Inst. Mech. Eng. Part H-J. Eng. Med. **228**(3), 287–296 (2014)
27. Tan, R., Liu, H., Li, H., Wang, Y.: Research on the critical sliding resistance on the quasi-static interaction between the capsule robot and the small intestine. Robot **36**(6), 704–710 (2014)
28. Zhang, C., Liu, H., Li, H.: Experimental investigation of intestinal frictional resistance in the starting process of the capsule robot. Tribol. Int. **70**, 11–17 (2014)
29. Zhang, C., Liu, H., Li, H.Y.: Modeling of frictional resistance of a capsule robot moving in the intestine at a constant velocity. Tribol. Lett. **53**(1), 71–78 (2014)
30. Baek, N.K., Sung, I.H., Kim, D.E.: Frictional resistance characteristics of a capsule inside the intestine for microendoscope design. Proc. Inst. Mech. Eng. [H] **218**(3), 193–201 (2004)

31. Liao, D.H., Zhao, J.B., Fan, Y.H., Gregersen, H.: Two-layered quasi-3D finite element model of the oesophagus. Med. Eng. Phys. **26**(7), 535–543 (2004)
32. Zhang, C., Liu, H., Su, G., Tan, R., Li, H.: Research of intestines' dynamic viscoelasticity based on five-element model. Gaojishu Tongxin/Chin. High Technol. Lett. **22**(9), 964–968 (2012)
33. Lyle, A.B., Luftig, J.T., Rentschler, M.E.: A tribological investigation of the small bowel lumen surface. Tribol. Int. **62**, 171–176 (2013)
34. Liu, Y., Pavlovskaia, E., Hendry, D., Wiercigroch, M.: Vibro-impact responses of capsule system with various friction models. Int. J. Mech. Sci. **72**, 39–54 (2013)
35. Gang, S., Cheng, Z., Renjia, T., Hongyi, L.: A design of the electromagnetic driver for the "internal force-static friction" capsubot. In: 2009 IEEE/RSJ International Conference on Intelligent Robots and Systems (IROS), 10–15 Oct 2009, pp. 613–617
36. Tan, R., Liu, H., Li, H., Wang, Y.: Dynamics analysis of the start motion of a capsule robot. Inf. Control **44**(5), 552–556 (2015)
37. Astrom, K.J., Canudas-De-Wit, C.: Revisiting the LuGre friction model stick-slip motion and rate dependence. IEEE Control Syst. Magn. **28**(6), 101–114 (2008)